protein being active in the GDP-bound state, we suppose that this complex, purified from cells, is derived from RacGTP:RhoGDI and that after GTP hydrolysis, RacGDP remains in the conformationally active state so long as it is bound to RhoGDI.
26. A. Hall and A. J. Self, *J. Biol. Chem.* **261**, 10963 (1986).
27. D. Diekmann *et al.*, *Nature* **351**, 400 (1991).
28. Y. Bromberg *et al.*, *J. Biol. Chem.* **269**, 7055 (1994).
29. We are grateful to the Cancer Research Campaign (United Kingdom) and the Medical Research Council (United Kingdom) (D.D. and A.H.) and to the Wellcome Trust (A.A. and A.W.S.) for their generous support.

7 April 1994; accepted 6 June 1994

14-3-3 Protein Homologs Required for the DNA Damage Checkpoint in Fission Yeast

Jon C. Ford, Fahad Al-Khodairy,* Eleftheria Fotou, Katherine S. Sheldrick,† Dominic J. F. Griffiths, Antony M. Carr‡

During the cell cycle, DNA is replicated and segregated equally into two daughter cells. The DNA damage checkpoint ensures that DNA damage is repaired before mitosis is attempted. Genetic studies of the fission yeast *Schizosaccharomyces pombe* have identified two genes, *rad24* and *rad25*, that are required for this checkpoint. These genes encode 14-3-3 protein homologs that together provide a function that is essential for cell proliferation. In addition, *S. pombe rad24* null mutants, and to a lesser extent *rad25* null mutants, enter mitosis prematurely, which indicates that 14-3-3 proteins have a role in determining the timing of mitosis.

A sophisticated series of controls has evolved that ensures the integrity of DNA before the initiation of mitosis. These controls include a checkpoint that prevents mitosis after DNA damage induced by radiation (*1*). A key unanswered question is how this radiation checkpoint interacts with the cell cycle machinery. Genetic analysis of *Schizosaccharomyces pombe* (reviewed in *2*) has identified two classes of radiation checkpoint mutants that are distinguishable by phenotype. The first class of mutants are defective in both the DNA damage checkpoint and in replication–mitosis dependency control (*3, 4*), and they carry mutations in any of six *rad-hus* genes. The second class are defective primarily in the DNA damage checkpoint (*4, 5*) and carry mutations in either the *chk1* or the *rad24* gene. Cells containing the *rad24.T1* mutation enter mitosis prematurely during normal growth, which indicates that the *rad24.T1* mutant may link the DNA damage checkpoint to the cell cycle machinery (*4*).

To investigate the defect in the *rad24.T1* mutant, we used an *S. pombe* genomic library (*6*) to isolate plasmids that complemented the cells' sensitivity to ultraviolet (UV) radiation. The complementing activity was localized to a 1.8-kb Eco RI–Bam HI fragment, and sequence analysis identified an open reading frame encoding a protein with 58% identity to the highly conserved eukaryotic 14-3-3 proteins (Fig. 1A). This sequence did not contain the *rad24* gene itself (*7*) but carried a multicopy suppressor of *rad24.T1*, which we designated *rad25*. Multicopy *rad25* plasmids completely suppressed the premature mitosis phenotype and the UV sensitivity of *rad24.T1* cells (*8*).

The 14-3-3 proteins have been identified in most eukaryotic cells (*9*) and diverse biochemical properties have been ascribed to them. Mammalian cells contain a minimum of seven 14-3-3 isoforms, and the single known *Saccharomyces cerevisiae* 14-3-3 homolog (BMH1) is nonessential (*10*). These observations suggested that functionally redundant 14-3-3 homologs might exist in *S. pombe*. To search for such homologs, we used degenerate primers corresponding to highly conserved sequences in the 14-3-3 proteins (Fig. 2) in polymerase chain reactions (PCRs). This analysis revealed two 14-3-3 genes, one of which was *rad25* (*11*). The predicted product of the second 14-3-3 gene (Fig. 1B) was 71% identical to that of *rad25*, and a null mutant had essentially the same phenotype as the *rad24.T1* mutant (Fig. 3). This gene mapped (*12*) to the same locus as the *rad24.T1* mutation and thus corresponds to the *rad24* gene. The *rad24-rad25* double null mutant was inviable (*13*), which indicates an essential role for the 14-3-3 homologs in *S. pombe*.

The *rad24* null cells were sensitive to UV and to ionizing radiation (Fig. 3, A and B), and quantitative analysis demonstrated that the duration of the delay to mitosis that was caused by DNA damage was reduced by one-half (Fig. 3C). This is an unusual phenotype for a null mutant of an *S. pombe* checkpoint gene (*3, 4*). We previously reported (*4*) that *rad24.T1* mutants show a mitotic catastrophe phenotype and die rapidly when DNA ligase function is disrupted by the temperature-sensitive *cdc17.K42* mutation, and that loss of *wee1* function in *rad24.T1* cells is lethal. Equivalent observations have been made with the *rad24* null mutant. In addition to these phenotypes, which have been linked to the loss of the radiation checkpoint pathway (*1, 5*), *rad24* null cells had a cytokinesis defect similar to that of *S. pombe* protein kinase C mutants (*14*); showed an unusual cone-shaped cell morphology (Fig. 4); and

A

```
MSNSRENSVYLAKLAEQAERYEEMVENMKKVACSNDKLSVEERNLLSVAY 50
KNIIGARRASWRIISSIEQKEESRGNTRQAALIKEYRKKIEDELSDICHD 100
VLSVLEKHLIPAATTGESKVFYYKMKGDYYRYLAEFTVGEVCKEAADSSL 150
EAYKAASDIAVAELPPTDPMRLGLALNFSVFYYEILDSPESACHLAKQVF 200
DEAISELDSLSEESYKDSTLIMQLLRDNLTLWTSDAEYNQSAKEEAPAAA 250
AASENEHPEPKESTTDTVKA
```

B

```
MSTTSREDAVYLAKLAEQAERYEGMVENMKSVASTDQELTVEERNLLSVA 50
YKNVIGARRASWRIVSSIEQKEESKGNTAQVELIKEYRQKIEQELDTICQ 100
DILTVLEKHLIPNAASAESKVFYYKMKGDYYRYLAEFAVGEKRQHSADQS 150
LEGYKAASEIATAELAPTHPIRLGLALNFSVFYYEILNSPDRACYLAKQA 200
FDEAISELDSLSEESYKDSTLIMQLLRDNLTLWTSDAEYSAAAAGGNTEG 250
AQENAPSNAPEGEREPKATHR
```

Fig. 1. Predicted sequences of *rad24* and *rad25* gene products (*21*). (**A**) The *rad25* gene was cloned as a multicopy suppressor of the *rad24.T1* mutant. A null allele was constructed by replacement of a 480–base pair Sph I fragment with a *ura4*$^+$ marker gene (*6*). The *rad25*::*ura4*$^+$ null mutant divided at a slightly reduced size, was mildly radiation-sensitive, and had a slight defect in the radiation checkpoint. (**B**) Fragments of the *rad24* gene were cloned by degenerate PCR (*11*) with different combinations of primers FTT1 (YTNYTNWSNGTNGCNTAYAARAA), FTT2 (TAYYTNAARATGAARGGNGAYTA), FTT3 (YTTCATYTTNTRRTARAANACYTT), and FTT4 (YTCRTARTARAANACNSWRAARTT) (Fig. 2). Thirteen FTT1-FTT2, five FTT3-FTT4, and six FTT1-FTT4 fragments were cloned and sequenced. Of these, seven were derived from *rad25* and seventeen defined a second gene, *rad24*. A null allele of *rad24* was constructed by introduction of a *ura4*$^+$ marker at the Bgl II site in the coding region (*6*). The *rad24*::*ura4*$^+$ null mutation maps to the same locus as, and produces a similar phenotype to, the *rad24.T1* mutation. The European Molecular Biology Laboratory database accession numbers for the DNA sequences are X79206 (*rad24*) and X79207 (*rad25*).

Medical Research Council Cell Mutation Unit, Sussex University, Falmer, Brighton BN1 9RR, UK.

*Present address: Research Centre (MBC 03), King Faisal Specialist Hospital, Riyadh 11211, Saudi Arabia.
†Present address: Department of Biochemistry and Molecular Biology, Stopford Building, Oxford Road, Manchester M13 9PT, UK.
‡To whom correspondence should be addressed.

Fig. 2. Alignment of the rad24, rad25, and BMH1 (*10*) amino acid sequences with that of the human 14-3-3 Zeta protein (*21, 22*). Dots indicate identity. The divergence between the *S. pombe* rad24 and rad25 proteins is less than that between the yeast and mammalian 14-3-3 homologs. The regions used to design the degenerate oligonucleotides for cloning of *rad24* are shown in bold (underlined, forward direction; overlined, reverse direction).

```
                                                                FTT1
14-3-3  M---DKNELVQKAKLAEQAERYDDMAACMKSVTEQGAELSNEERNLLSVA
rad24   .STTSREDA.YL.........EG.VEN....ASTDQ..TV.........
rad25   .SN-SRENS.YL......R...EE.VEN..K.ACSNDK..V.........
BMH1    .ST-SREDS.YL.........EE.VEN..T.ASS.E...V.........

14-3-3  YKNVVGARRSSWRVVSSIEQKTEGAEK---KQQMAREYREKIETELRDIC
rad24   ....I....A...I.......E.SKGNTA-QVELIK...Q...Q..DT..
rad25   ...II....A...II......E.SRGNTR-QAALIK...K...D..S...
BMH1    ....I....A...I.....E.E.SK..SEHEVELICS..S......TK.S

                                  FTT3      FTT2
14-3-3  NDVLSLLEKFLIPNASQAESKVFYLKMKGDYYRYLAEVAAGDDKKGIVDQ
rad24   Q.I.TV...H.....AS.......Y.............F.V.EKRQHSA..
rad25   H....V...H...A.TTG......Y.............FTV.EVC.EAA.S
BMH1    D.I..V.DSH...S.TTG......Y......HH....FSS..AREKATNA

                                                        FTT4
14-3-3  SQQAYQEAFEISKKEMQPTHPIRLGLALNFSVFYYEILNSPEKACSLAKT
rad24   .LEG.KA.S..ATA.LA.......................DR..Y...Q
rad25   .LE..KA.SD.AVA.LP..D.M.................D...S..H...Q
BMH1    .LE..KT.S..ATT.LP.....................Q...D...H.R.Q

14-3-3  AFDEAIAELDTLSEESYKDSTLIMQLLRDNLTLWTSDTQGDEAEAGEGGE
rad24   ......S...S.........................AEYSA.A..GNT.
rad25   V.....S...S.........................AEYNQSAKE.APA
BMH1    ...D...............................MSESGQAEDQQQQ

14-3-3  N
rad24   GAQENAPSNAPEGEREPKATHR
rad25   AAAASENEHPEPKESTTDTVKA
BMH1    QQHQQQQPPAAAEGEAPK
```

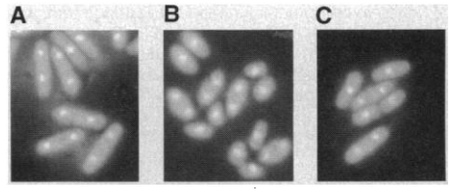

Fig. 4. Morphology and cell size at division. Photographs of (**A**) wild-type, (**B**) *rad24* null, and (**C**) *rad25* null *S. pombe* cells during exponential growth, illustrating the semi-*wee* and unusual cone-shaped cell morphology phenotypes. The average cell length at septation was estimated for *rad24::ura4*, *rad25::ura4*, and the isogenic wild-type strain sp011 (*24*) by averaging 20 random measurements. Wild-type, 14.7 μm; *rad24*, 9.7 μm; *rad25*, 12.6 μm. Gene replacement of the *rad13* (excision repair) locus (*25*) in strain sp011 did not result in a semi-*wee* phenotype.

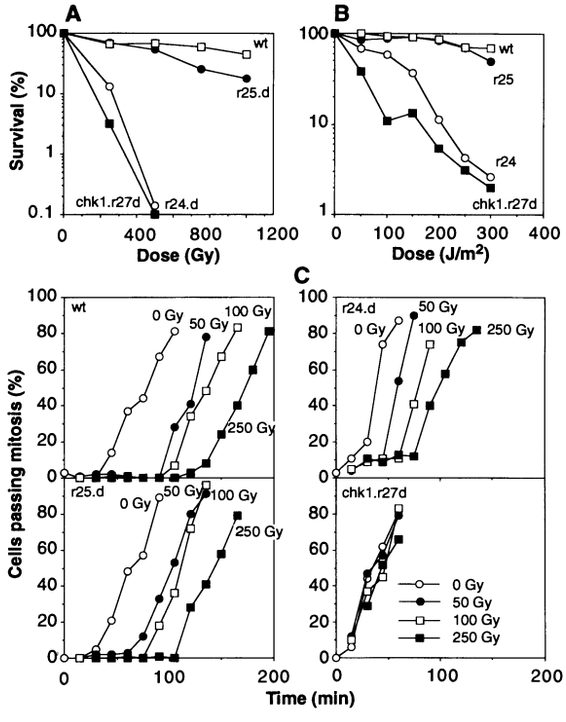

Fig. 3. Survival analysis of *S. pombe rad24* (r24.d), *rad25* (r25.d), and *chk1* (chk1.r27d) (*4*) null mutants after exposure to gamma (**A**) or UV (**B**) radiation. We tested the gamma sensitivity of cells synchronized in G_2 (*23*) by irradiating samples in suspension before plating. We tested the UV sensitivity of cells synchronized in G_2 (*23*) by plating 10^3 cells and immediately irradiating the plates at the appropriate dose. The *chk1* null cells were included as a control that has lost the radiation checkpoint (*4*). (**C**) Radiation checkpoint measurements in wild-type and in *rad24* (r24.d), *rad25* (r25.d), and *chk1* (chk1.r27d) null mutants. Cells were synchronized (*23*), and G_2 cells were inoculated into yeast extract media. The culture was split into four parts and irradiated in a Gammacell 1000 ^{137}Cs source (Nordion, Ontario, Canada) (dose rate, 12 Gy min^{-1}). At 15-min intervals, cell samples were fixed in methanol and were later examined by 4,6-diamino-2-phenylindole (DAPI) and Calcofluor staining (*4*) to determine the fraction of cells that had undergone mitosis. Both *rad24* and *rad25* null mutants were reproducibly deficient in the duration of the delay to mitosis after irradiation. The *chk1* mutant completely lacked a delay to mitosis in this assay. Comparison of the checkpoint deficiencies and the radiation sensitivities of the *chk1* and *rad24* null cells indicates that a further response to gamma radiation, distinct from the G_2 delay defect, may be deficient in *rad24* null cells.

entered mitosis prematurely, which resulted in a small cell size at division (known as a semi-*wee* phenotype).

In contrast to the *rad24* null mutant, the *rad25* null mutant had only marginal (but reproducible) effects on resistance to irradiation and on the duration of mitotic arrest after irradiation (Fig. 3, A, B, and C). It also showed only a slight decrease in cell size at division (Fig. 4). The *rad25* null cells did not display synthetic lethality with *cdc17* or *wee1* mutants, were not defective in cytokinesis, and did not assume an unusual cell morphology. It is possible that, like the essential function, the *rad24* and *rad25* checkpoint functions overlap. If so, this could account for the unusual hypomorphic phenotype of the *rad24* null mutant. Both *rad24* and *rad25* mRNAs were easily detectable in blots of total RNA and were not induced after DNA damage (*15*).

It has been proposed that *chk1* links the DNA damage checkpoint pathway to the *cdc2*-encoded protein kinase (*5*), but thus far there is no direct evidence to support this. We overexpressed *chk1* in wild-type *S. pombe* cells, using an inducible promoter (*16*), and found that the cells elongated, did not enter mitosis, and consequently did not form colonies. The same phenotype of cell cycle arrest was seen with the *rad-hus* mutants *rad1°*, *rad3.dR3*, *rad9.d*, *rad17.d*, *rad26.d*, and *hus1.14*; thus, these genes are likely to lie upstream of *chk1* in the DNA damage checkpoint pathway. In contrast, overexpression of *chk1* in *rad24.d* null cells resulted in less cell elongation and less inhibition of mitosis (*17*) and did not prevent colony formation. These data are consistent with the hypothesis that *rad24* acts downstream of *chk1* in the DNA damage checkpoint (*17*).

Members of the 14-3-3 family possess numerous biochemical activities (reviewed in 9), including a role in the Ca^{2+}-dependent activation of enzymes involved in neurotransmitter synthesis (*18*), the ability to regulate the activity of protein kinase C (*19*), and an association with polyomavirus middle tumor antigen during transformation (*20*). These data, plus the phenotype of the *rad24* and *rad25* null mutants, suggest a role for 14-3-3 proteins in signal transduction pathways. The identification of a genetic phenotype in yeast should facilitate functional analysis of these proteins.

REFERENCES AND NOTES

1. L. H. Hartwell and T. A. Weinert, *Science* **246**, 629 (1989); T. Enoch and P. Nurse, *Cell* **65**, 921 (1991).
2. K. S. Sheldrick and A. M. Carr, *Bioessays* **15**, 775 (1993).
3. F. Al-Khodairy and A. M. Carr, *EMBO J.* **11**, 1343 (1992); R. Rowley, S. Subramani, P. G. Young, *ibid.*, p. 1335; T. Enoch, A. M. Carr, P. Nurse, *Genes Dev.* **6**, 2035 (1992).
4. F. Al-Khodairy *et al.*, *Mol. Biol. Cell* **5**, 147 (1994).
5. N. Walworth, S. Davey, D. Beach, *Nature* **363**, 368 (1993).
6. N. C. Barbet, W. J. Muriel, A. M. Carr, *Gene* **114**, 59 (1992).

7. The complementing plasmid (*rad25*) was integrated and four independent strains were crossed to *rad*$^+$ *ura*$^-$ cells. For each strain, approximately 20% of *rad*$^-$ *ura*$^-$ segregants were generated, which suggests that integration had occurred at a locus distinct from *rad24.T1*. As was consistent with this possibility, crosses between the *rad25* null mutant and the *rad24.T1* mutant yielded progeny that were approximately 30% *rad*$^+$.
8. Overexpression of *rad25*, even from a high-level expression vector, resulted in only a slight increase in cell length at division. Similar observations have been made with *rad24*.
9. A. Aitken *et al.*, *Trends Biochem. Sci.* **17**, 498 (1992).
10. G. P. H. van Heusden, T. J. Wenzel, E. L. Lagendijk, H. Y. de Steensma, J. A. van den Berg, *FEBS Lett.* **302**, 145 (1992).
11. Four degenerate PCR primers (Fig. 2) were used in amplification reactions on genomic *S. pombe* DNA. Three different pairs of the primers were used to generate distinct DNA fragments. Representative DNAs from each of these fragments were cloned and sequenced. Analysis of 24 independent clones suggested that *S. pombe* contained two 14-3-3 homologs. One of these was *rad25*. The entire coding region of the second 14-3-3 homolog was isolated as follows: Genomic DNA was digested with Hind III and recircularized. Polymerase chain reaction was done with primers pointing away from each other, thus amplifying (to the nearest Hind III site) the unknown sequences that flank the original fragment. The amplified regions contained the 3′ end of the coding region but not the entire 5′ end. To obtain the 5′ coding region, we performed anchored PCR on a complementary DNA (cDNA) library template with one primer that was unique to the known coding region and one primer that was designed to hybridize to the vector region flanking the 5′ end of the insert. Finally, we amplified the entire region, including the intron, by PCR from genomic DNA and sequenced two independent clones with synthetic primers.
12. When the *rad24* null mutant was crossed with the *rad24.T1* mutant, no wild-type recombinants were observed among 5×10^3 progeny.
13. To test the viability of the double mutant, we dissected 24 tetrads from a cross between the *rad24* and *rad25* null mutants to obtain four spores. Seven tetrads segregated four colonies (two *rad24::ura*$^+$ and two *rad25::ura*$^+$), eleven tetrads segregated three colonies (one *rad*$^+$ *ura*$^-$, one *rad24::ura*$^+$, and one *rad25::ura*$^+$), and six tetrads segregated two colonies (two *rad*$^+$ *ura*$^-$).
14. T. Toda, M. Shimanuki, M. Yanagida, *EMBO J.* **12**, 1987 (1993).
15. K. S. Sheldrick and A. M. Carr, unpublished data.
16. K. Maundrell, *J. Biol. Chem.* **265**, 10857 (1990); G. Basi, E. Schmid, K. Maundrell, *Gene* **123**, 131 (1993).
17. Wild-type cells containing the *chk1* cDNA in the REP1 vector (*16*) were shifted to a medium without thiamine in order to induce expression of *chk1*. The cells elongated and mitosis was reduced to a rate at which colonies did not form. Cell mass accumulation continued. After 24 hours, the average cell length was 42 μm (cells containing only the empty vector divided at 13.9 μm). Under identical circumstances, *rad24* null mutant cells continued to divide (but at a reduced rate), and colonies formed in approximately twice the time required for control cells containing the empty vector. This indicated that an appreciable rate of cell division had occurred. After 24 hours, cells were only partially elongated, with an average cell length of 22.3 μm at division (cells containing only the empty vector divided at 9.3 μm). The *rad25* null mutants behaved like wild-type cells when *chk1* was overexpressed (cells were 42 μm in length after 24 hours). When *chk1* overexpression was reduced by use of the REP41 vector (*16*), both *rad24* and *rad25* cells could form large colonies, whereas the growth of wild-type cells was still impeded. Although we cannot eliminate the possibility that *rad24* and *rad25* activate *chk1*, these results are consistent with the idea that the 14-3-3 function acts downstream of *chk1*.
18. T. Ichimura *et al.*, *Proc. Natl. Acad. Sci. U.S.A.* **85**, 7084 (1988).
19. A. Aitken, C. A. Ellis, A. Harris, L. A. Sellers, A. Toker, *Nature* **344**, 594 (1990); T. Isobe *et al.*, *FEBS Lett.* **308**, 121 (1992).
20. D. C. Pallas *et al.*, *Science* **265**, 535 (1994).
21. Abbreviations for the amino acid residues are as follows: A, Ala; C, Cys; D, Asp; E, Glu; F, Phe; G, Gly; H, His; I, Ile; K, Lys; L, Leu; M, Met; N, Asn; P, Pro; Q, Gln; R, Arg; S, Ser; T, Thr; V, Val; W, Trp; and Y, Tyr.
22. L. A. Zupan, D. L. Steffens, C. A. Berry, M. Landt, R. W. Gross, *J. Biol. Chem.* **267**, 8707 (1992).
23. N. C. Barbet and A. M. Carr, *Nature* **364**, 824 (1993).
24. J. M. Murray *et al.*, *Nucleic Acids Res.* **20**, 2673 (1992).
25. A. M. Carr *et al.*, *ibid.* **21**, 1345 (1993).
26. We thank A. Lehmann for valuable discussions and B. Edgar and C. Norbury for the *S. pombe* cDNA library. Supported in part by Commission of the European Community contract F13P-CT920007. F.A.K. was supported by the Saudi Arabian government.

7 March 1994; accepted 20 May 1994

Association of Polyomavirus Middle Tumor Antigen with 14-3-3 Proteins

David C. Pallas,* Haian Fu, Leda C. Haehnel,† Wendy Weller,‡ R. John Collier, Thomas M. Roberts

To carry out its transformation function, the middle tumor antigen (MT) of murine polyomavirus associates with a number of cellular proteins involved in regulation of cell proliferation, including pp60$^{c\text{-}Src}$, phosphatidylinositol 3-kinase, protein phosphatase 2A, Src homologous and collagen protein and growth factor receptor–binding protein 2. Here, two additional MT-associated proteins were identified as members of the 14-3-3 family of proteins. Yeast homologs of 14-3-3 proteins have recently been shown to play a role in the timing of mitosis. Thus, regulation of 14-3-3 protein function by MT may contribute to the development of neoplasia.

The primary transforming protein of murine polyomavirus is MT, a membrane protein with no known enzymatic activity (*1*). MT is thought to transform cells and induce tumors in animals by virtue of its association with cellular proteins involved in the control of cell proliferation. These proteins include pp60$^{c\text{-}Src}$ and other members of the Src family of protein-tyrosine kinases (*1*), phosphatidylinositol 3–kinase (*2*), two subunits of protein phosphatase 2A (*3*), Src homologous and collagen protein (SHC) (*4*), and growth factor receptor–binding protein 2 (GRB2) (*4*).

Among the MT-associated proteins that remain to be characterized are two with molecular masses of 27 and 29 kD (*5*). As is the case for the protein phosphatase 2A subunits, the 27- and 29-kD proteins associate efficiently with baculovirus-expressed polyomavirus MT in insect cells (Fig. 1, A and B) (*6*). To identify these proteins, we purified them from human 293 cells by preparative two-dimensional isoelectric focusing/SDS-polyacrylamide (2D) gels and subjected them to microsequence analysis (*7*). The sequences of multiple tryptic peptides (Table 1) indicated that both proteins belong to the 14-3-3 family of proteins; the 29-kD protein corresponds to the epsilon subspecies of 14-3-3 proteins, whereas the 27-kD protein appears to be a mixture of several 14-3-3 subspecies. This family of proteins was originally thought to be brain-specific and to function as a coregulator of tryptophan and tyrosine hydroxylases (*8*). Subsequently, these proteins have been found in a wide variety of mammalian tissues and in other eukaryotic organisms including plants and yeast and have had a number of activities ascribed to them (*8*).

The identity of these proteins was confirmed by immunoblot analysis of MT immunoprecipitates with an antibody raised to a peptide sequence conserved within several 14-3-3 subspecies (*9*). The antibody detected a 27-kD protein in MT immunoprecipitates prepared from mouse NIH 3T3 cells stably expressing MT (Fig. 1, C and D) (*10*). This same antibody recognized the 27-kD but not the 29-kD protein from cell lysates (*11*). This result is consistent with the fact that the peptide used as immunogen is not well conserved in the epsilon subspecies of 14-3-3 proteins.

The 14-3-3 proteins are an obligatory

D. C. Pallas, L. C. Haehnel, W. Weller, T. M. Roberts, Division of Cellular and Molecular Biology, Dana-Farber Cancer Institute, and Department of Pathology, Harvard Medical School, Boston, MA 02115, USA.
H. Fu and R. J. Collier, Department of Microbiology and Molecular Genetics and Shipley Institute of Medicine, Harvard Medical School, Boston, MA 02115, USA.

*To whom correspondence should be addressed.
†Present address: Endogen Inc., 640 Memorial Drive, Cambridge, MA 02139, USA.
‡Present address: Department of Health and Human Services, Public Health Service, Office of the Assistant Secretary for Health, Washington, DC 20201, USA.